ACS OMEGA

Open Access

http://pubs.acs.org/journal/acsodf

Article

Using a New Fe_3O_4@CPAM Magnetic Flocculant and Microwave to Demulsify Heavy Oil-in-Water Emulsions

Published as part of ACS Omega virtual special issue "Magnetic Nanohybrids for Environmental Applications".

Nana Sun,* Huina Sun, Jianbo Hu, Shiqi Xu, Lisha Shen, and Yuli Ma

Cite This: *ACS Omega* 2024, 9, 9202−9215

Read Online

ACCESS | Metrics & More | Article Recommendations

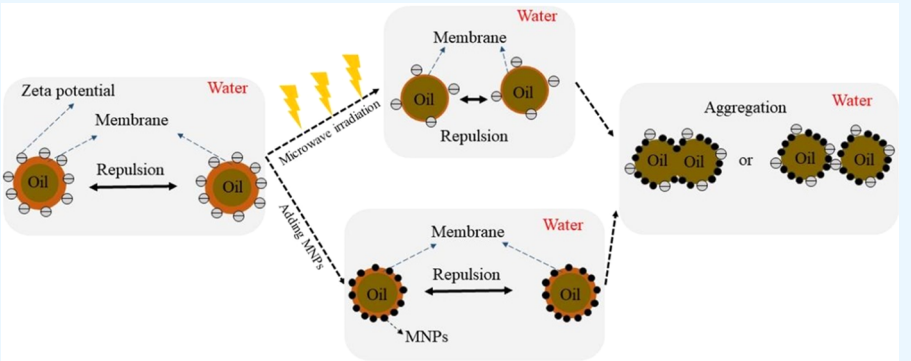

ABSTRACT: In this study, cationic polyacrylamide (CPAM)-coated magnetic nanoparticles (MNPs) Fe_3O_4@CPAM were synthesized for treating heavy O/W emulsions. This Fe_3O_4@CPAM was characterized by Fourier transform infrared spectroscopy (FTIR), X-ray diffraction (XRD), thermogravimetric analysis (TGA), and vibrating sample magnetometry (VSM) techniques, and its synergistic performances with microwaves were evaluated in detail with respect to the microwave radiation power, radiation time, and magnetic nanoparticle concentration. On this basis, the distribution of oil droplets and the wettability and chargeability of magnetic nanoparticles were measured without or with microwave radiation using biomicroscopy, contact angle measurement instrument, and a ζ-potential analyzer, thus revealing the synergistic demulsification mechanism between microwave and magnetic nanoparticles. The results showed that excessively high or low microwave radiation parameters had an inhibitory effect on the magnetic nanoparticle demulsification, and microwave promoted the magnetic nanoparticle demulsification only when the radiation parameters were in the optimal range. In addition, the water separation rate showed an increasing and then decreasing trend with the increase of magnetic nanoparticles concentration, with or without microwave action. As an example, the water separation rate of the emulsion for 1 h was 21.34% when the Fe_3O_4 concentration was 175 mg/L without microwave action, while it increased to 55.56% with microwave action. In contrast, when the concentration of Fe_3O_4@CPAM was 175 mg/L, the water separation rate was 42.86% without microwave radiation, while it was further increased to 77.38% under microwave radiation. These results indicate that magnetic nanoparticles and their complexes significantly affect the water separation process under different conditions. There is a more obvious coupling synergistic effect between Fe_3O_4@CPAM and microwave. This was due to the lower absolute potential of Fe_3O_4@CPAM and its higher hydrophobicity.

1. INTRODUCTION

To improve oil recovery, chemical flooding has been adopted in major oil fields in recent years. Natural active agents make crude oil emulsions more complex in composition and more stable kinetically.[1] The accompanying problem is that demulsification is more difficult, and the water content of oil must be less than 0.5% before exporting. Therefore, achieving demulsification efficiently and environmentally has always been a concern of the oil industry.

At present, the chemical demulsification method has been widely used, and it has a series of characteristics, such as fast processing speed and a wide application range. The processing of demulsifiers increases the difficulty, and some demulsifiers themselves have certain toxicity, which has a harmful effect on the environment.[2]

Received: October 19, 2023
Revised: January 13, 2024
Accepted: January 19, 2024
Published: February 15, 2024

Microwaves are high-frequency electromagnetic waves that not only have the characteristics of strong penetration, fast speed, and large volume but also can solve the problem of environmental pollution. Microwave demulsification has attracted extensive attention from scholars in recent years. Sun et al.[3] investigated the effects of microwave irradiation, conventional heating, and microwave chemistry methods on heavy oil−water separation. The results showed that water separation first increased and then decreased with an increasing microwave irradiation time. And when the microwave power was improved, the water separation first increased sharply and then increases slowly. Lv et al.[4] studied the influences of microwave heating temperature and power on the distribution of particle size and demulsification efficiency of oily sludge. The results showed that the demulsification temperature of oily sludge should be kept at 77 °C. The demulsification efficiency of oily sludge showed a trend of first increasing and then decreasing with the increase of microwave heating temperature and power. In addition, microwave irradiation can simultaneously reduce the demulsification temperature, demulsification time, and centrifugation speed, proving that microwave irradiation is a fast, efficient, and low-cost demulsification method. Binner et al.[5] used the microwave method to break a water-in-oil emulsion. The results showed that microwave heating was beneficial to water droplet aggregation and coalescence. At the same time, microwave heating results in an order of magnitude improvement in the separation time. The study by Martínez-Palou et al.[6] showed that with the increase of microwave power, the demulsification efficiency was improved. However, the application of microwave demulsification alone often fails to meet the standard of dehydration.

In recent years, the use of functionalized magnetic nanoparticles (MNPs) as demulsifiers has attracted considerable attention. Magnetite Fe_3O_4 is one of the most commonly used magnetic nanoparticles because of its low cytotoxicity and good biocompatibility. In addition, MNPs often need to be modified with active substances to improve their interfacial activity and dispersibility.

This magnetic demulsifier can adsorb at the oil/water interface and impart magnetic properties to the dispersed droplets. Under an applied magnetic field, the droplets marked by magnetic demulsification can be rapidly coalesced and separated from the continuous phase. Ali et al.[7] synthesized and characterized a magnetic nanoparticle (P(MMA-AA-DVB)/Fe_3O_4) with interfacial activity and magnetic responsiveness using direct polymerization of soap-free emulsions and solvothermal techniques, illustrated good interfacial activity of the magnetic nanoparticles, and found that the magnetic nanoparticles made the interfacial properties stable and responded rapidly to the applied magnetic field, allowing the separation of heavy oil emulsions within 1 h. Liang et al.[8] investigated the magnetic demulsification of diluted crude O/W nanoemulsions using oleic acid-coated magnetite nanoparticles under the effect of an applied magnetic field. With increasing Fe_3O_4@OA dosage, the demulsification efficiency was increased. The demulsification efficiency was related to the wettability of the magnetic nanoparticles, and when the water contact angle was 90°, the demulsification efficiency reached a maximum value. Xu et al.[9] modified expanded perlite (EP) with 3-aminopropyltriethoxysilane (APTES) to form EP@APTES and then grafted magnetic Fe_3O_4 nanoparticles (NPs) onto the surface of EP@Fe_3O_4 to synthesize a novel EP@APTES-Fe_3O_4 composite. The synthesized composites were used as a magnetic demulsifier to treat emulsified wastewater. The results showed that the composites were easy to be synthesized and recovered, have good demulsification performance, and provide a promising and cost-effective emulsion breaker for the removal of oil from wastewater. Zhao et al.[10] synthesized polyethylenimine-coated ferric tetroxide magnetic nanoparticles (MNPs) using a one-step thermal solvent method and used these MNPs to O/W emulsions for demulsification studies. The results showed that the synthesized MNPs could successfully adsorb on the oil−water interface of the emulsion, thus causing rapid destabilization of oil droplets by applying a magnetic field.

It is known from previous studies that magnetic nanoparticles can effectively achieve oil−water separation and the magnetic nanoparticles can be recovered by an applied magnetic field for multiple recyclings after demulsification. Considering that microwave radiation can generate high-frequency electromagnetic fields and that magnetic nanoparticles adsorbed on the surface of oil droplets will make the oil droplets electromagnetic, there is a coupling interaction between microwaves and magnetic nanoparticles, but domestic and foreign research on this aspect is still limited.

In view of this, based on previous experiments by our group, first, a new Fe_3O_4@CPAM magnetic flocculant was synthesized by coating cationic polyacrylamide CPAM on the surface of Fe_3O_4 using a water-soluble method, and the synthesized functionalized magnetic nanoparticles were characterized by various processes. Second, this magnetic flocculant was applied to heavy O/W emulsions as a demulsifier in cooperation with microwaves (MWs), the relationship between its demulsification efficiency and microwave radiation power, microwave radiation time, and concentration of magnetic nanoparticles was investigated in detail, and the microscopic mechanism of microwave−magnetic nanoparticle synergistic demulsification was revealed.

2. EXPERIMENTAL SECTION

2.1. Materials and Methods. Heavy crude oil was obtained from the Xinjiang oil field in Urumchi, China. The density is equal to 964.0 kg·m^{-3} at 25 °C. The physical and chemical properties of the heavy crude oil are shown in Table 1. And the viscosity−temperature curve of heavy crude oil is presented in Figure 1.

Table 1. Physical and Chemical Properties of Xinjiang Heavy Crude Oil

resins (wt %)	asphaltenes (wt %)	sulfur content (wt %)	water content (vol %)
26.78	15.12	1.86	0.50

All of the other chemicals were of analytical grade, including triiron tetroxide (Fe_3O_4), sodium bisulfite ($NaHSO_3$), acrylamide (AM), and methacryloyloxyethyl trimethylammonium chloride (DMC), which were provided by Aladdin Chemistry (Shanghai, China). Anionic polyacrylamide (HPAM) was purchased from the Tianjin Damao Chemical Reagent Factory. Emulsifier (OP-10) and gelatin were acquired from Tianjin Fuyu Fine Chemical Co. Citric acid was purchased from Tianjin Baishi Chemical Co. Ammonium persulfate ($(NH_4)_2S_2O_8$) was provided by Tianjin Zhiyuan Chemical Reagent Co.

2.2. Synthesis of CPAM and Fe_3O_4@CPAM. *2.2.1. Synthesis of CPAM.* A certain amount (15% monomer mass ratio) of acrylamide (AM) and an equal amount of methacryloylox-

https://doi.org/10.1021/acsomega.3c08238
ACS Omega 2024, 9, 9202−9215

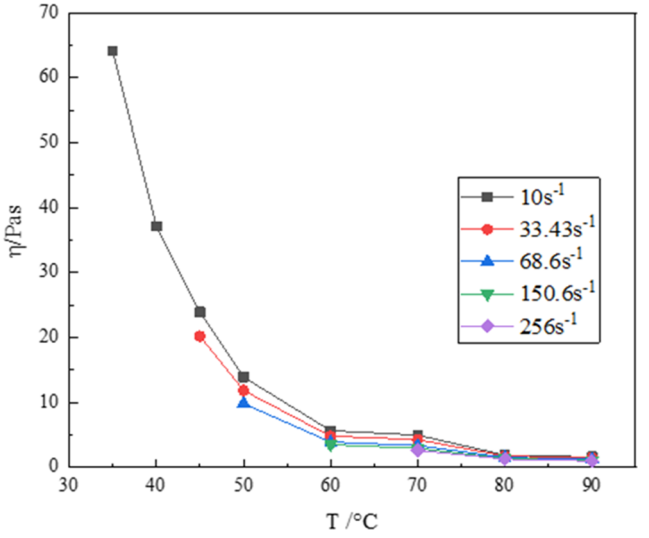

Figure 1. Viscosity−temperature curve of heavy crude oil.

yethyl trimethylammonium chloride (DMC) were weighed, and then a certain amount of deionized water was added and poured into a three-necked flask that was fixed with an iron stand and placed in a constant-temperature water bath to achieve the polymerization initiation temperature of 40 °C at a pH of 7. Then, nitrogen was passed through the mixture for 30 min, and 0.3% ammonium persulfate was added to the reaction mixture dropwise for 5 min. The reaction was initiated by adding sodium bisulfite solution and holding the mixture for 3 h. A transparent colloid was obtained. The cationic polyacrylamide gel was removed, dried, cut with scissors, soaked in acetone for 24 h, and then soaked in anhydrous ethanol for 24 h to remove the homopolymer and residual monomer. The obtained white solid was placed in a dish, dried in a constant-temperature drying oven, and crushed after drying to obtain powdered polyacrylamide.

2.2.2. Synthesis of Fe_3O_4@CPAM. A certain amount (15% by mass of monomer) of acrylamide (AM) and equal amounts of methacryloyloxyethyl trimethylammonium chloride (DMC), ferric tetroxide, gelatin, and citric acid were weighed and added

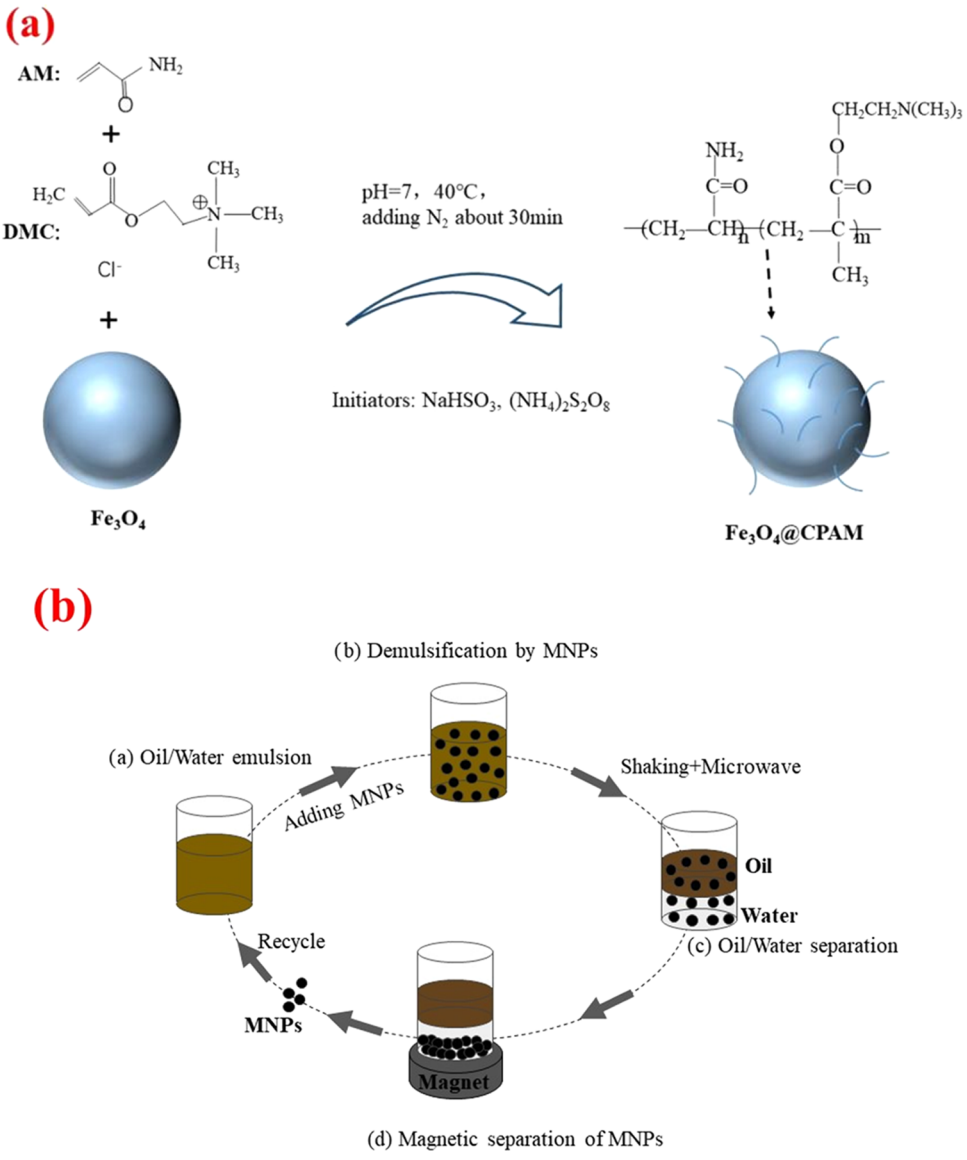

Figure 2. (a) Synthetic scheme of Fe_3O_4@CPAM MNPs and (b) schematic illustration of demulsification and recycling tests.

https://doi.org/10.1021/acsomega.3c08238
ACS Omega 2024, 9, 9202−9215

to a certain amount of deionized water; this mixture was then poured into a three-necked flask and fixed with a wire stand in a constant-temperature water bath so that the polymerization system could reach the initiation temperature of 40 °C at pH = 7, and nitrogen gas was passed through the mixture for 30 min. The reaction was initiated by adding 0.3% (by mass of monomer) ammonium persulfate dropwise for 5 min, and then, sodium bisulfite solution was added for 3 h to obtain a transparent colloid. The colloid was removed, and the cationic polyacrylamide colloid was dried and cut with scissors. The colloid was soaked in acetone for 24 h and then in anhydrous ethanol for 24 h to remove the homopolymer and residual monomer. The obtained black solid was placed in a dish, dried in a constant-temperature drying oven, removed, and crushed after drying to obtain the powdered polyacrylamide sample. The synthesis procedure is illustrated in Figure 2. The diagram of the preparation device is illustrated in Figure 3.

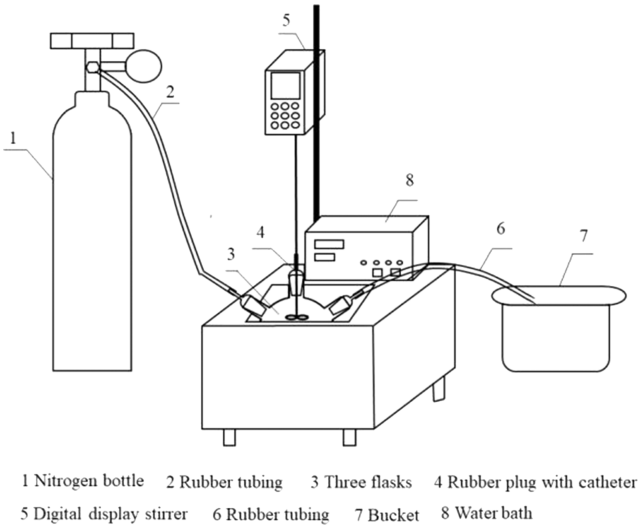

Figure 3. Diagram of the Fe_3O_4@CPAM preparation device.

2.3. Preparation of the Emulsion. 1.5% OP-10 and 0.15% HPAM were formulated into binary active water as emulsifier solutions used in this experiment. The heavy oil and the active water-containing emulsifier were mixed at a mass ratio of 6:4 and allowed to stand in a constant-temperature water bath at 25 °C for 30 min. Then, the above mixture was stirred at a speed of 1000 rpm, and the stirring time was 3 min to complete the emulsion preparation.

2.4. Demulsification Test. *2.4.1. Magnetic Nanoparticle Demulsification.* The magnetic nanoparticles were prepared in a masterbatch at a concentration of 1000 mg/L, ultrasonically dispersed, and the emulsion was weighed on an electronic balance. Then, the magnetic nanoparticle solution was added into the emulsion drop by drop using a disposable syringe, and the sample was poured into a stoppered colorimetric tube and shaken 200 times to evenly disperse the magnetic nanoparticles in the emulsion.

2.4.2. Microwave-Magnetic Nanoparticle Demulsification. The emulsion with added magnetic nanoparticles was poured into a 250 mL two-necked round-bottom flask and placed into an MAS-II microwave synthesis/extraction reaction workstation under atmospheric pressure. According to the experimental plan, different microwave radiation parameters were set for the microwave treatment and the temperature was controlled by an infrared temperature control device.

After the microwave treatment was completed, the emulsion was poured into a colorimetric tube and placed in a constant-temperature water bath at 70 °C. For the first 10 min, the height of separated water was measured every 2 min, and the height was recorded every 10 min. After 1 h of measurement, the samples were left in a water bath for 24 h. The total height of the emulsion in the colorimetric tube was measured after 24 h.

2.5. Calculation of the Water Separation Rate. The bottle test method was used to determine the water separation rate of the emulsions under different conditions. The higher the water separation rate, the better the demulsification effect. The water separation rate is calculated as shown in eq 1

$$f = \frac{V_1}{V_2} \times 100\% = \frac{H_1}{H_2 \times 40\%} \times 100\% \quad (1)$$

where f is the demulsification water separation rate, %; V_1 is the volume of the dispensed water, mL; V_2 is the volume of the total water, mL; H_1 is the height of the dispensed water, mm; and H_2 is the total height of the emulsion, mm.

2.6. Characterization. *2.6.1. Oil Droplet Distribution.* The distribution of oil droplets in water phase was observed by a biological microscope (Malvern Instruments Ltd., U.K.), which was equipped with a 45× objective lens with 4000 × 3000 pixel image resolution. The shapes and sizes of the oil droplets were recorded with a Sony digital camera. The steps were as follows.

To prepare emulsions with different radiation parameters and magnetic nanoparticles, the emulsion was extracted by using disposable syringes, dropped onto a slide, covered with a coverslip, and the appearance of the emulsion was observed by microscopy.

2.6.2. ζ-Potentials of Magnetic Nanoparticles. The ζ-potentials of different magnetic nanoparticles were measured by a Zetasizer Nano-ZS (Malvern Instruments Ltd., U.K.) at 25 °C using a 15 mW helium−neon laser as the incident beam. The steps were as follows.

The magnetic nanoparticles were prepared into a certain concentration of mother liquor and ultrasonicated for 40 min, and after microwave treatment at different radiation powers, 1 mL of the sample was added to the ζ-potential cuvette using a rubber-tipped dropper. Then, the ζ-potential was measured by using a Malvern particle size analyzer. Each sample was measured five times, and the results were averaged.

2.6.3. Wettability of Magnetic Nanoparticles. Wettability of the magnetic nanoparticles was measured by a contact meter (JC2000D2). The volume of the liquid was set at 3 μL, and the contact angle was calculated by the five-point fitting method. The specific steps were as follows.

The magnetic nanoparticles were added to a certain concentration of solution and ultrasonically dispersed for 40 min at room temperature. The above solution was coated onto glass slides to form a dense and uniform film and was dried in a vacuum oven at 50 °C for 12 h. Then, a drop of deionized water was dropped onto the slides to measure the contact angle. Each sample surface was measured five times, and the results were averaged.

2.6.4. XRD, FTIR, TGA, and VSM. X-ray powder diffraction patterns were obtained by an X-ray diffractometer (XRD, SHIMADZ, XRD-6100, Japan) using Cu Kα radiation in the 2θ range of 10−80°.

Fourier transform infrared spectra were recorded with a Fourier transform infrared spectrometer (FTIR, Nicolet iS50,

https://doi.org/10.1021/acsomega.3c08238
ACS Omega 2024, 9, 9202−9215

Thermo Fisher). A small amount of the prepared sample was mixed with potassium bromide, ground into a powder, pressed, and placed in a Fourier transform infrared spectrometer to analyze its structure and to observe and derive the infrared spectrum.

Thermal properties were measured by thermogravimetric analysis (TGA, METTLER, Switzerland) under a nitrogen atmosphere at a heating rate of 10−800 °C.

Magnetic properties were measured by using a vibrating sample magnetometer (VSM, model Lake Shore, Lakeshore 7404) at room temperature.

3. RESULTS AND DISCUSSION

3.1. Characterization of Fe_3O_4 and Fe_3O_4@CPAM.

3.1.1. XRD. The structures of Fe_3O_4, CPAM, and Fe_3O_4@CPAM MNPs were revealed by X-ray diffraction, and the results are shown in Figure 4.

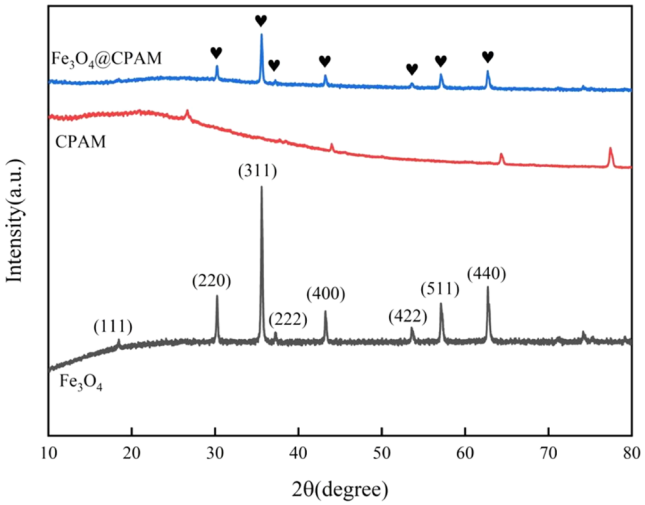

Figure 4. XRD patterns of CPAM, Fe_3O_4, and Fe_3O_4@CPAM MNPs.

Fe_3O_4 nanoparticles showed six characteristic diffraction peaks at 2θ = 18.4, 30.2, 35.7, 43.5, 53.7, 57.4, and 62.9°, which correspond to the (111), (220), (311), (222), (400), (422), (511), and (440) lattice planes.[1111] These lattice planes are the standard pattern for crystalline magnetite with a spinel structure. The characteristic diffraction peak of Fe_3O_4@CPAM was almost identical to that of Fe_3O_4, which demonstrated that Fe_3O_4 was successfully incorporated with CPAM. CPAM has a broad diffuse diffraction peak in the range of 10−30°. Compared with CPAM, the diffraction peak of Fe_3O_4@CPAM was slightly wider, indicating the existence of a nonmagnetic and amorphous CPAM-coating on the surface of Fe_3O_4.[12]

3.1.2. FTIR. The chemical structures of Fe_3O_4, CPAM, and Fe_3O_4@CPAM MNPs were obtained by FTIR spectroscopy, as shown in Figure 5.

It can be seen from Figure 5 that the bending vibration absorption peaks of CPAM were mainly sourced from AM and DMC. The absorption band of CPAM at 3457 cm^{-1} was assigned to the $-NH_2$ group of AM. The peaks at 1663 and 1453 cm^{-1} were ascribed to the stretching of C═O and the stretching vibration of C−N in the amide groups, respectively. The characteristic peak at 953 cm^{-1} was attributed to the quaternary ammonium cationic group $-N^+(CH_3)_3$ of DMC.[13] For the naked Fe_3O_4 particles, the absorption peaks at approximately 570 cm^{-1} were derived from the Fe−O bond of the bulk

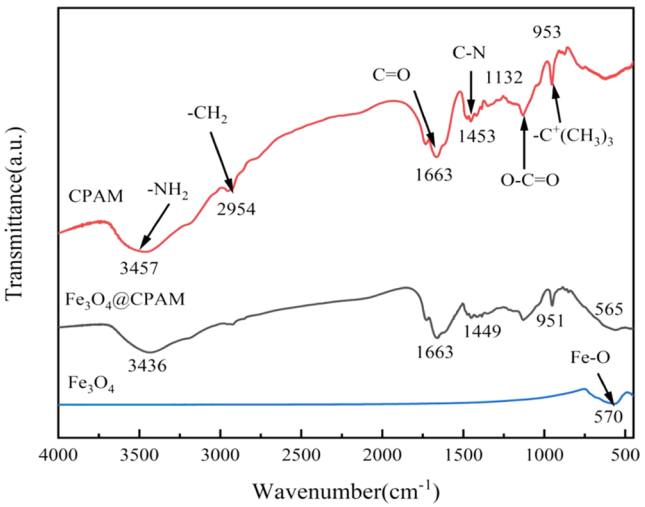

Figure 5. FTIR spectra of CPAM, Fe_3O_4, and Fe_3O_4@CPAM MNPs.

magnetite.[14] All characteristic peaks were present in Fe_3O_4@CPAM. Consequently, these results proved that CPAM was adsorbed onto the Fe_3O_4 nanoparticles.

3.1.3. TGA. To determine the successful coating between Fe_3O_4 and CPAM, TGA curves of Fe_3O_4 and Fe_3O_4@CPAM were compared, and the results are displayed in Figure 6.

Figure 6a shows that the TGA curve of Fe_3O_4 has two stages. In the first stage, the weight loss of 0.3% within the range of 20−200 °C was due to the evaporation of absorbed water on particle surfaces.[15] In the second stage, the weight loss of 0.6% within the range of 250−400 °C was due to the gradual oxidation in air. As shown in the TGA (Figure 6b) curve of Fe_3O_4@CPAM, there were also three stages. In the first stage, a weight loss of 8.63% was observed within the range of 20−150 °C. In the second stage, a weight loss of 20.35% occurred at 200−300 °C, which was caused by the decomposition of amide groups, imidation, and breakage of intermolecular hydrogen bonds formed by some amide groups.[16] In the third stage, a weight loss of 19.56% occurred at 300−450 °C, which was caused by the thermal decomposition of CPAM. All of the evidence and discussion of thermal gravimetric characterization indicated that Fe_3O_4@CPAM was successfully synthesized.

3.1.4. VSM. The magnetic properties of the synthesized MNPs were investigated by PPMS at room temperature. The magnetic hysteresis loops of Fe_3O_4 and Fe_3O_4@CPAM are shown in Figure 7.

As shown in Figure 7, the saturation magnetization of Fe_3O_4 nanoparticles was 1.46 emu/g, which was slightly larger than that of Fe_3O_4@CPAM (0.33 emu/g). The decreased magnetization for Fe_3O_4@CPAM was attributed to the coating of cationic polyacrylamide on the surface of the magnetic nanoparticles.[17]

3.2. Demulsification Performance of Fe_3O_4 and Fe_3O_4@CPAM.

The magnetic nanoparticles selected in this study were Fe_3O_4 and Fe_3O_4@CPAM, and their mass concentration was 175 mg/L. These emulsions with various types of magnetic nanoparticles were separately subjected to conventional heating and microwave radiation demulsification. The microwave irradiation power was 400 W, and the microwave irradiation time was 20 s. The experimental results are shown in Figure 8.

Figure 8 shows that the water separation rates of MW, Fe_3O_4, Fe_3O_4@CPAM, Fe_3O_4 + MW, and Fe_3O_4@CPAM + MW were

https://doi.org/10.1021/acsomega.3c08238
ACS Omega 2024, 9, 9202−9215

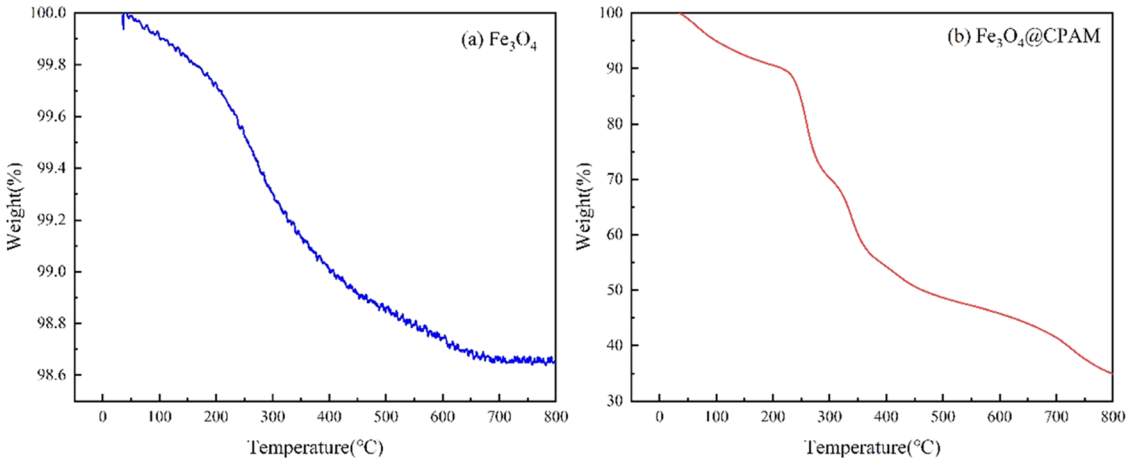

Figure 6. TGA curves of (a) Fe_3O_4 and (b) Fe_3O_4@CPAM MNPs.

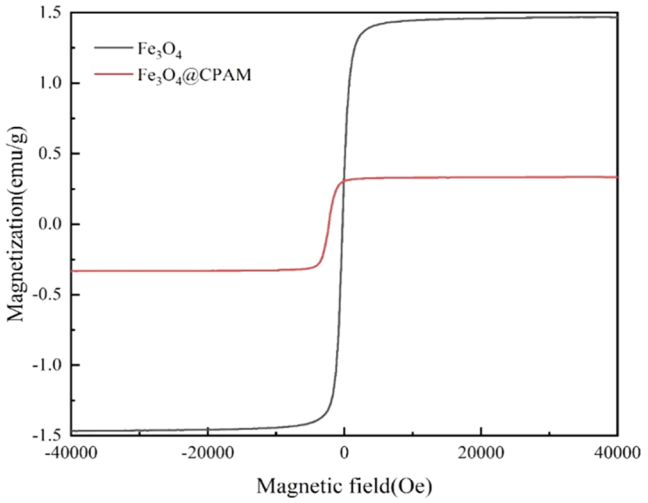

Figure 7. Magnetization curves of Fe_3O_4 and Fe_3O_4@CPAM MNPs.

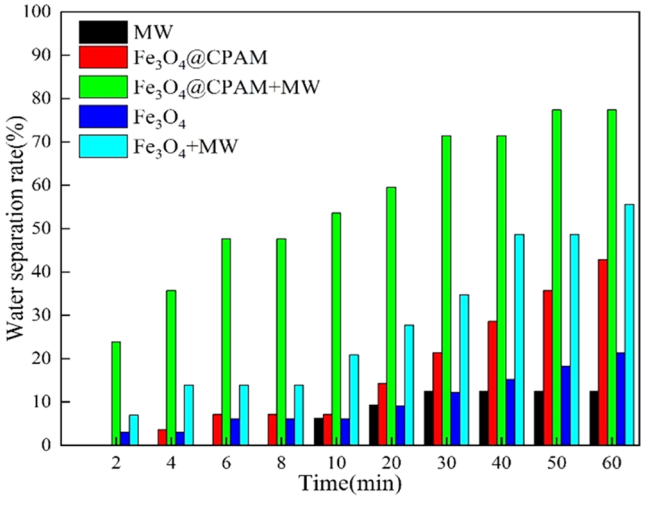

Figure 8. Effect of the experimental conditions on the demulsification efficiency.

12.5, 21.34, 42.86, 55.56, and 77.38%, respectively. Without microwave action, the water separation rate of Fe_3O_4@CPAM was 21.52% higher than that of Fe_3O_4. And under microwave radiation, the water separation rate of Fe_3O_4@CPAM was 33.92% higher than that of Fe_3O_4. The above results indicated that microwaves had more obvious synergistic effects with modified magnetic nanoparticles.

The reasons for this phenomenon included the following points. (1) Fe_3O_4@CPAM adsorbed on the surface of the oil droplet could form a mixed film structure with coexisting magnetic nanoparticles and surfactant, which reduced the stability of emulsions. (2) As shown in Table 2, the absolute values of ζ-potential were in the order Fe_3O_4 > Fe_3O_4 + MW > Fe_3O_4@CPAM > Fe_3O_4@CPAM + MW; therefore, the electrostatic repulsion force between oil droplets reached the lowest value under the coupling effect of microwave and modified magnetic nanoparticles Fe_3O_4@CPAM. (3) It also can be seen from Table 2 that the order of the contact angle was Fe_3O_4@CPAM + MW > Fe_3O_4@CPAM > Fe_3O_4 + MW > Fe_3O_4, so the hydrophobic interaction of magnetic nanoparticles was the strongest with the action of microwave.

In addition, the modified magnetic nanoparticle Fe_3O_4@CPAM was easy to replace the original surfactant adsorbed on the oil−water interface, which made the interfacial film arrangement loose and reduced the mechanical strength of the interfacial film. On the other hand, the polymeric flocculant can act as a sweeping net to allow the oil beads to sediment.

At the same time, under microwave radiation, the electromagnetic energy should be converted to thermal energy, which resulted in the increase of the emulsion temperature. As the temperature increased, the thermal movement of the magnetic polymer macromolecules was intense and the flocculation between oil droplets was enhanced.

3.3. Effect of Radiation Power on Demulsification of Fe_3O_4 and Fe_3O_4@CPAM.

3.3.1. Demulsification Performance. Radiation power is an important factor affecting the demulsification of microwave-magnetic nanoparticles. For these experiments, the concentration of both Fe_3O_4 and Fe_3O_4@CPAM was 175 mg/L, the radiation time was 20 s, and the radiation power was selected as 100−700 at 100 W intervals. The experimental results were compared to the blank experiments without microwave treatment, as shown in Figure 9.

Figure 9A shows that the water separation rate of the emulsion first increased and then decreased with increasing radiation power. In the range of microwave radiation power of 100−700 W within 10−40 min, the water separation rate was higher than that of simple Fe_3O_4 without microwave action, and the highest water separation rate of 500 W was 72.92%. After 40 min, only the water separation rate of the emulsion with a microwave

https://doi.org/10.1021/acsomega.3c08238
ACS Omega 2024, 9, 9202−9215

Table 2. Parameters of Magnetic Nanoparticles under Different Conditions

	Fe_3O_4	Fe_3O_4 + MW	Fe_3O_4@CPAM	Fe_3O_4@CPAM + MW
water separation rate (%)	21.34	55.56	42.86	77.38
ζ-potential (mV)	−30.1	−29.7	−21.5	−21.06
contact angles (deg)	23.21	41.1	42.11	55.69

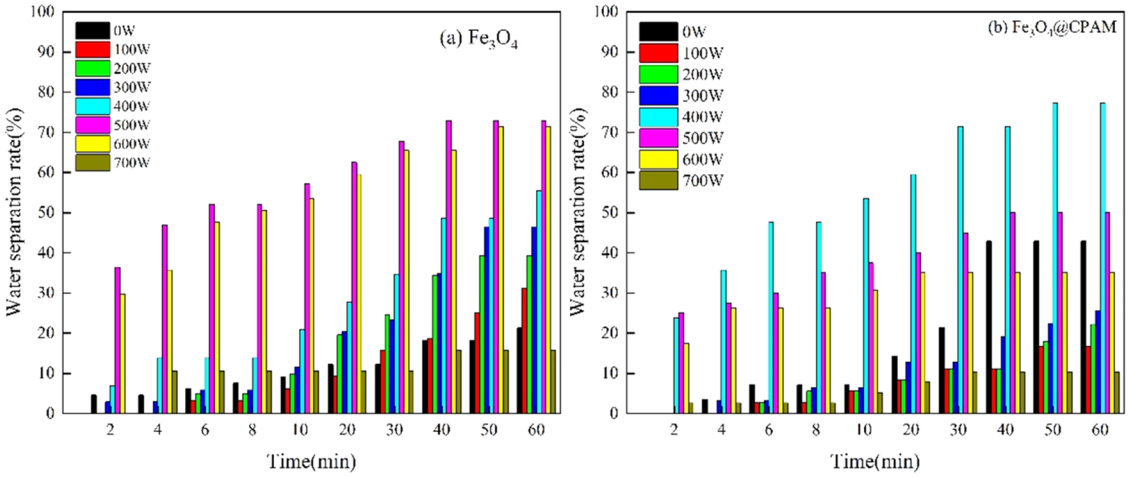

Figure 9. Effect of radiation power on the demulsification of heavy O/W emulsions: (a) Fe_3O_4 and (b) Fe_3O_4@CPAM.

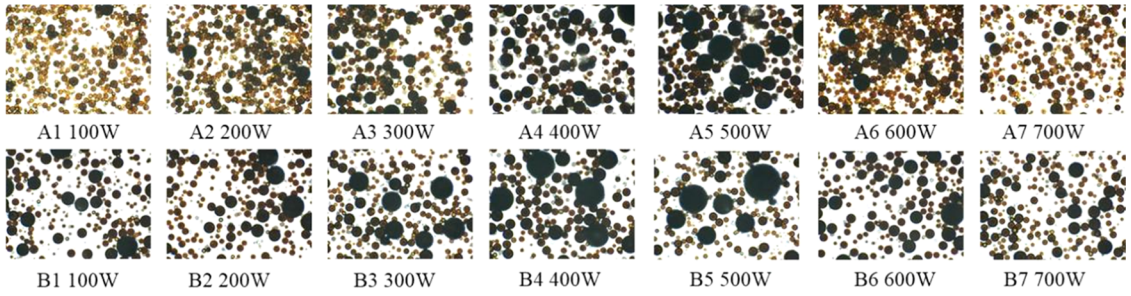

Figure 10. Effect of the radiation power on the oil droplet distribution (A1−A7 show the effects of Fe_3O_4 MNPs, while B1−B7 show the effects of Fe_3O_4@CPAM MNPs).

radiation power of 700 W was lower than that of the individual Fe_3O_4 magnetic nanoparticles without microwave radiation.

Figure 9B shows that when the radiation power was increased, the water separation rate first improved and then decreased, with the maximum rate achieved at 400 W. In the range of microwave radiation powers of 100−400 and 700 W from 6 to 40 min, the water separation rate was lower than that of simple Fe_3O_4@CPAM magnetic nanoparticles without microwave radiation, and the water separation rate of the emulsion reached a maximum value of 53.57% at 400 W. After 40 min, when the microwave radiation power was 400−500 W, the water demulsification efficiency was higher.

The following conclusions can be obtained by combining Figure 9A with B. Under the same microwave conditions (400 W, 20 s), Fe_3O_4@CPAM had a 21.82% higher water separation rate than Fe_3O_4 in 1 h, indicating that the synergistic effect of Fe_3O_4@CPAM and microwave demulsification was better than that of Fe_3O_4.

In summary, either too high or too low of a microwave radiation power inhibited magnetic nanoparticle demulsification; however, in the optimal radiation power range, microwaves played a synergistic role in magnetic nanoparticle demulsification. In addition, the coupling effect between Fe_3O_4@CPAM and microwave was stronger than that of Fe_3O_4.

3.3.2. Demulsification Mechanism. 3.3.2.1. Distribution of Oil Droplets. To further elucidate the mechanism of the influence of the radiation power on the coalescence of oil droplets for different demulsification methods, microscopy images of oil droplets were obtained for the comparative analysis. The results are shown in Figure 10.

Figure 10 shows that when only magnetic nanoparticles were used, as the microwave radiation power increased, the oil droplet size first increased and then decreased and the number of oil droplets first became less and then more. When the microwave radiation power was 500 and 400 W, the number of oil droplets was the lowest, and the size was the largest.

The reason for the above phenomenon was that Fe_3O_4 has magnetic response characteristics, and the emulsion droplets adsorbed with Fe_3O_4 were rapidly deflected under the action of the electromagnetic field, which in turn leads to collision between oil droplets, and the small droplets in the water phase quickly gathered into large droplets (as shown in Figure 10A1−A5,10B1−B4). In addition, magnetic nanoparticles, as a high dielectric loss material, have strong adsorption properties, and when they were adsorbed onto the surface of dispersed droplets, the electromagnetic loss factor of the emulsion system increased, which in turn enhanced the ability of the emulsion to absorb microwaves. As the radiation power increases, more energy was

https://doi.org/10.1021/acsomega.3c08238
ACS Omega 2024, 9, 9202−9215

absorbed by emulsion, leading to an increase in the emulsion temperature. Thus, the Brownian motion of oil droplets was accelerated, which promoted the coalescence of droplets, and the high temperature expanded the gap between adjacent interfacial molecules by weakening the interaction force. As the temperature increases, the thermal movement of magnetic polymer macromolecules was intense, and the flocculation between oil droplets and between oil droplets and the magnetic flocculant was enhanced. In addition, there was a nonthermal effect of microwaves: Microwave radiation generated high-frequency electromagnetic waves, and with the change in electromagnetic field, polar water molecules and charged droplets rapidly rotated to produce charge displacement. Therefore, the double electric layer was destroyed, weakening the ζ-potential of the emulsion so that the diffusion layer was thinner, and the electrostatic repulsion force between dispersed droplets was reduced. The higher the microwave radiation power, the stronger the neutralization effect of the applied electric field on the ζ-potential of the oil droplet surface, and the higher the emulsion breaking efficiency.

However, when the radiation power exceeded the optimal radiation power, the water separation rate decreased with increasing radiation power. This is because, on the one hand, too high power will lead to the desorption of magnetic nanoparticles and the weakening of the electromagnetism of the oil droplets.[18,19] On the other hand, excessive temperatures can lead to violent collisions between droplets,[20−23] and the already aggregated large droplets collide with each other to form small droplets (as shown in Figure 10A6,A7,10B5−B7). In addition, with an increasing electric field strength, an electrical dispersion phenomenon will occur, affecting the dewatering efficiency and causing a loss of electrical energy.

3.3.2.2. ζ of Magnetic Nanoparticles. Considering the charge characteristics of magnetic nanoparticles will directly affect the demulsification efficiency, Fe_3O_4@CPAM powder with the strongest microwave coupling effect was selected as an example. The results are shown in Figure 11.

As shown in Figure 11, the absolute potential of Fe_3O_4@CPAM first decreased and then increased. When the microwave radiation power was increased from 100 to 300 W, the absolute value of the ζ-potential decreased from 34.87 to 21.93 mV, and both were higher than those of Fe_3O_4@CPAM without microwave treatment. When the power was set from 400 to 500 W, the absolute potential value increased from 21.06 to 21.33 mV, which was lower than that of Fe_3O_4@CPAM without microwave treatment. When the microwave radiation power was improved from 600 to 700 W, the absolute value of the potential of Fe_3O_4@CPAM increased from 27.77 to 28.83 mV, and both were higher than those of Fe_3O_4@CPAM without microwave treatment. The potential of Fe_3O_4@CPAM without the microwave treatment was −21.5 mV.

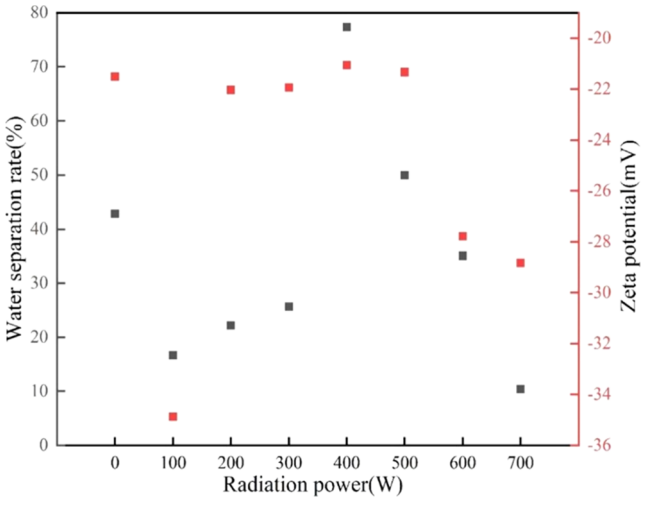

Figure 11. Influence of the microwave radiation power of Fe_3O_4@CPAM MNPs on the ζ-potential.

Considering that the OP-10 emulsifier used in this experiment is a nonionic surfactant and HPAM is an anionic polyacrylamide, when these surfactants were adsorbed on the oil−water interface, the oil droplets of the emulsion were negatively charged. Although Fe_3O_4@CPAM has a certain negative charge, it has a small size effect and a surface effect, so it can overcome the electrostatic repulsion between oil droplets and is attached to the oil−water interface. When the radiation power was increased, the decrease in the absolute value of the potential resulted in a reduction of the repulsive potential energy between oil droplets. When the microwave radiation power was further increased, the absolute value of the potential increased, leading to greater electrostatic repulsion between oil droplets and between magnetic nanoparticles and oil droplets. At a microwave radiation power of 400 W, the absolute value of the Fe_3O_4@CPAM potential reached a minimum of 21.06 mV. At this time, the electrostatic repulsion was the weakest, which was most favorable to the aggregation of oil droplets.

3.3.2.3. Wettability of Magnetic Nanoparticles. The wettability of magnetic nanoparticles affects their adsorption capacity; therefore, this study investigated the effect of different radiation powers on the contact angle of magnetic nanoparticles. The radiation power ranged from 100 to 700 W at intervals of 100 W. Fe_3O_4@CPAM powder with the strongest microwave coupling effect was selected as an example, and the results are presented in Figure 12.

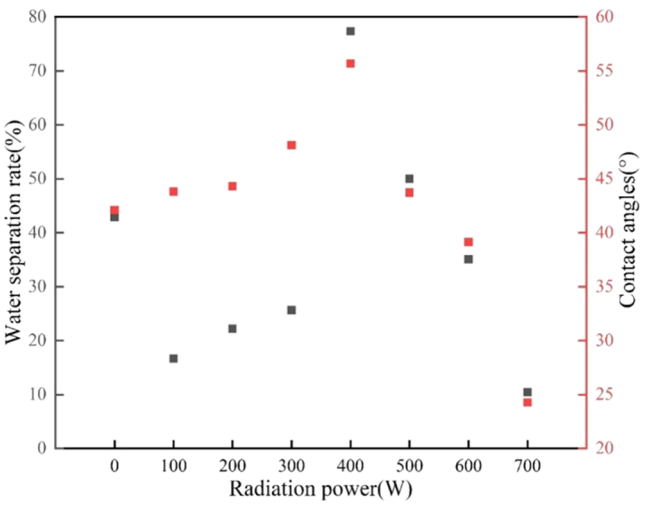

Figure 12. Influence of the microwave radiation power on the contact angles.

Figure 12 shows that with improving microwave radiation power, the contact angle of the magnetic nanoparticles initially increased and then decreased. Without microwave treatment, the contact angle of Fe_3O_4@CPAM was 42.11°. When the radiated power was improved from 100 to 400 W, the contact angles for Fe_3O_4@CPAM increased from 43.82 to 55.69°, and

https://doi.org/10.1021/acsomega.3c08238
ACS Omega 2024, 9, 9202−9215

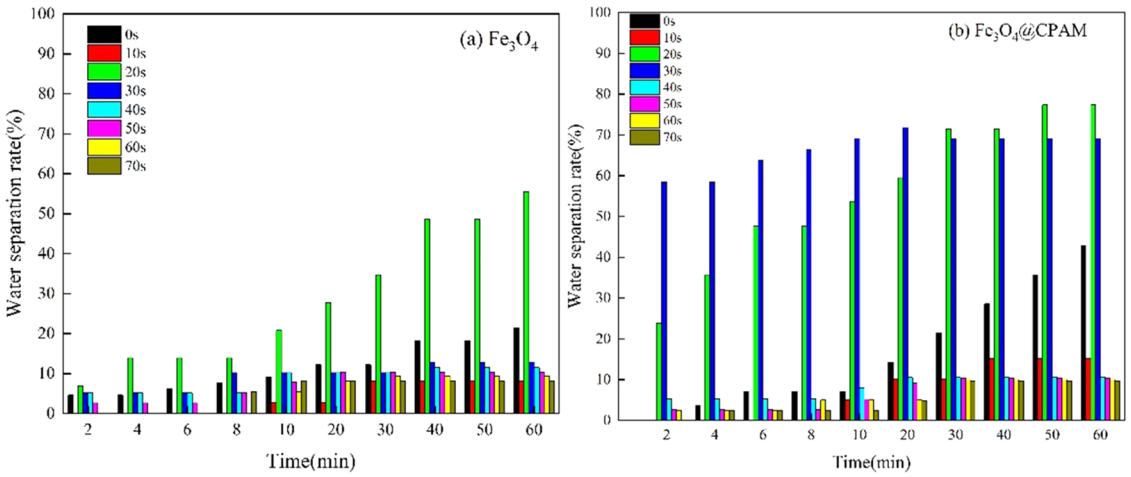

Figure 13. Effect of the radiation time on the demulsification of the heavy O/W emulsion: (a) Fe_3O_4 and (b) Fe_3O_4@CPAM.

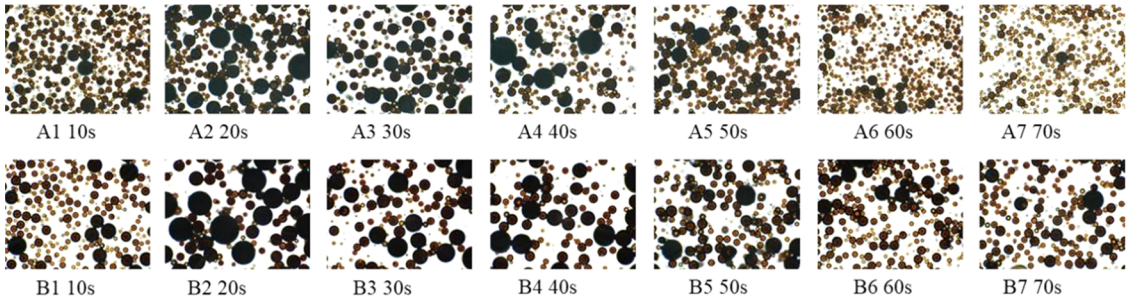

Figure 14. Effect of the radiation time on the oil droplet distribution: (a) Fe_3O_4 and (b) Fe_3O_4@CPAM (A1−A7 show the effects of Fe_3O_4 magnetic nanoparticles, while B1−B7 show the effects of Fe_3O_4@CPAM magnetic nanoparticles).

when the radiated power became 400−700 W, the contact angles for Fe_3O_4@CPAM decreased from 55.69 to 43.73°. The contact angle of Fe_3O_4@CPAM corresponding to the optimal radiation power of 400 W had a maximum value of 55.69°.

The reason for the above phenomenon was that under the action of microwave radiation, the high-speed rotation of polar water molecules can break the hydrogen bonds between water molecules, and the ability to break hydrogen bonds was enhanced as the microwave radiation power. The number of hydrogen bonds decreased and its hydrophobic effect was enhanced, which was conducive to the adsorption of magnetic nanoparticles onto the oil−water interface,[24] thereby forming a mixed interface film, leading to a reduction in the mechanical strength of the interface film. With a further increase in the radiation power, the hydrophilicity of Fe_3O_4@CPAM was stronger and their adsorption capacity on the interface became weaker, which was not helpful for demulsification.

3.4. Effect of Radiation Time on Demulsification Using Fe_3O_4 and Fe_3O_4@CPAM. *3.4.1. Demulsification Performance.* In this section, Taking Fe_3O_4 and Fe_3O_4@CPAM as examples, the concentration was 175 mg/L. The influence of the radiation time on the demulsification of magnetic nanoparticles was determined, and the radiation time was set to be 10−70 at 10 s intervals. The experimental results were compared with the blank without microwave treatment; the experimental results are presented in Figure 13.

Figure 13A shows that within 10−20 min, the microwave irradiation time was 20−40 s, and the water separation rate of the emulsion was higher than that of pure Fe_3O_4 magnetic nanoparticles without microwave radiation. The water separation rate reached the highest value of 27.78% when the microwave irradiation time was 20 s. After 20 min, only when the microwave irradiation time was 20 s, the demulsification efficiency was higher than that of the magnetic nanoparticles without microwave irradiation, and the maximum value was 55.56%.

Figure 13B shows that the water separation rate of emulsions at microwave radiation times of 10 and 40−50 s was higher than that of pure magnetic nanoparticles throughout the 1 h, with the best water separation effect at a radiation time of 20 s, and the highest water separation rate reached 77.38%.

At the same time, the following conclusions can be drawn in conjunction with Figure 9A,9B. Under the same microwave conditions (400 W, 20 s), Fe_3O_4@CPAM had a 21.82% higher water separation rate than Fe_3O_4 in 1 h. The synergistic effect of Fe_3O_4@CPAM and microwave demulsification was more obvious than that of Fe_3O_4.

In summary, a microwave radiation time that is too long or too short will inhibit the demulsification of the magnetic nanoparticle. Only in the optimal radiation time range, there is the coupling action between microwave and magnetic nanoparticles, and the synergistic effect of Fe_3O_4@CPAM and microwave on demulsification is stronger than that of Fe_3O_4.

3.4.2. Demulsification Mechanism. 3.4.2.1. Distribution of Oil Droplets. To further elucidate the mechanism of the influence of the radiation time on the coalescence of oil droplets for different demulsification methods, microscopy images of the oil droplets were used for comparative analysis. The results are shown in Figure 14.

https://doi.org/10.1021/acsomega.3c08238
ACS Omega 2024, 9, 9202−9215

Figure 14 shows that with the extension of the microwave radiation time, the number of oil droplets first decreased and then increased and the oil droplet size initially became larger and then smaller. When the microwave irradiation time was 20 s, the number of dispersed droplets was the lowest, and the size was the largest.

The reasons for these results are as follows: A longer microwave radiation duration meant that more electromagnetic energy would be dissipated by the microwave, and according to the law of the conservation of energy, more thermal energy is converted by the medium, resulting in an increase in the emulsion temperature.[25] On the one hand, an increase in temperature accelerated the Brownian motion of liquid droplets, which facilitated their flocculation, aggregation, and coalescence. On the other hand, the solubility of the interfacial active material in the water or oil phase was improved with increasing temperature, subsequently reducing the adsorptive capacity of the O/W interface and leading the interfacial film to become thinner.[25] The thermal motion of the magnetic polymer macromolecules was intense, and the flocculation is strengthened. In addition, the attractive force of adjacent molecules was weakened, causing the interfacial film structure to become looser. As the temperature increased, the thermal movement of magnetic nanoparticles was intensified and they were more likely to migrate to the oil−water interface, thus forming a mixed film structure.

However, the interfacial film had a certain mechanical strength that did not result in the complete coalescence of oil droplets as the temperature increased further; at the same time, overheating led to a violent collision between the adjacent molecules. Therefore, when the microwave radiation time was too long, the number of oil droplets became more, and its size became smaller.

3.4.2.2. ζ of Magnetic Nanoparticles. The charge carried by magnetic nanoparticles affects the charge and chargeability of oil droplets in both a positive and negative manner, and in view of this, the effect of different radiation times on the ζ-potential of the magnetic nanoparticles was investigated. Fe_3O_4@CPAM was selected for the experiments, and the radiation time ranged from 10 to 70 s with a time interval of 10 s. The experimental results are shown in Figure 15.

Figure 15 shows that with increasing irradiation time, the absolute value of the ζ-potential of Fe_3O_4@CPAM first decreased and then increased. When the microwave irradiation time increased from 10 to 20 s, the absolute value of the ζ-potential decreased from 27.27 to 21.06 mV, and only the ζ-potential at 10 s was higher than that of the magnetic nanoparticles without microwave irradiation. When the microwave irradiation was increased from 30 to 70 s, the absolute potential of Fe_3O_4@CPAM increased from 23 to 29.15 mV, which were higher than the ζ-potential of magnetic nanoparticles without microwave treatment. When the microwave irradiation was 20 s, the absolute value of the ζ-potential of Fe_3O_4@CPAM reached the lowest value of 21.06 mV.

Considering that the emulsifier OP-10 used in this experiment was a nonionic surfactant and HPAM was an anionic polyacrylamide, when the emulsion was stabilized, the oil droplets were negatively charged. Fe_3O_4@CPAM has a certain negative charge, but because of the small size effect and surface effect of the magnetic nanoparticles themselves, Fe_3O_4@CPAM can overcome the electrostatic repulsion between oil droplets to adsorb onto the oil−water interface. When the microwave irradiation time was prolonged, the absolute potential of the magnetic nanoparticles decreased, resulting in a decrease in the amount of charge, and the repulsive potential energy between the oil droplets was weakened. When the microwave irradiation time was further prolonged, the absolute value of the ζ-potential of the magnetic nanoparticles became higher, resulting in an increase in the electrostatic repulsion. When the microwave irradiation time was 20 s, the absolute potential of Fe_3O_4@CPAM reached a minimum of 21.06 mV. At this time, the electrostatic repulsion between oil droplets was the weakest, and this was most conducive to oil droplets aggregation.

3.4.2.3. Wettability of Magnetic Nanoparticles. The wettability of magnetic nanoparticles determines their adsorption capacity on the oil−water interface.[26] Based on this, the effects of microwave radiation times on the contact angles of magnetic nanoparticles were investigated in this section, with radiation times ranging from 10 to 70 s and time intervals of 10 s. The results are shown in Figure 16.

Figure 16 shows that the contact angle of Fe_3O_4@CPAM first became larger and then smaller with increasing microwave radiation time. The contact angle of pure Fe_3O_4@CPAM was

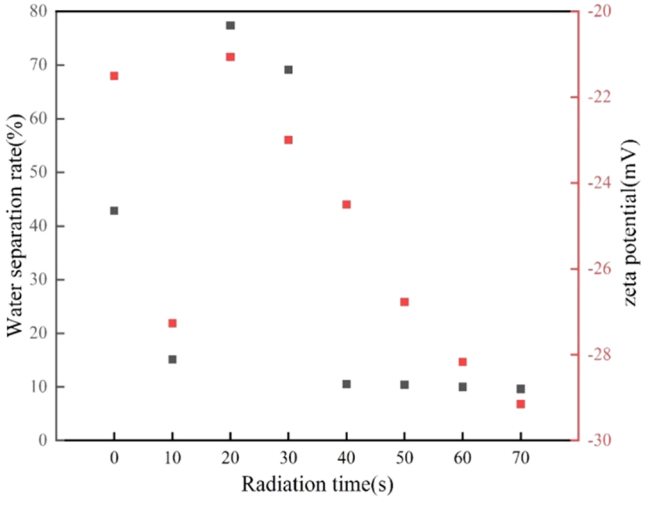

Figure 15. Influence of the microwave radiation time on the ζ-potential of Fe_3O_4@CPAM.

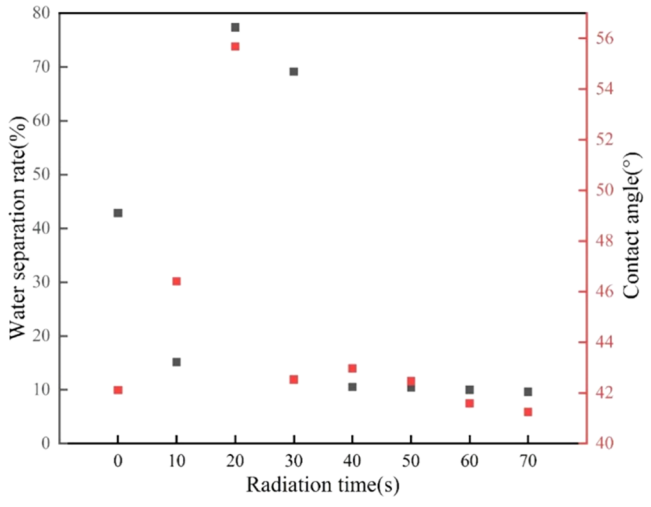

Figure 16. Influence of microwave radiation time on the contact angle of Fe_3O_4@CPAM.

https://doi.org/10.1021/acsomega.3c08238
ACS Omega 2024, 9, 9202−9215

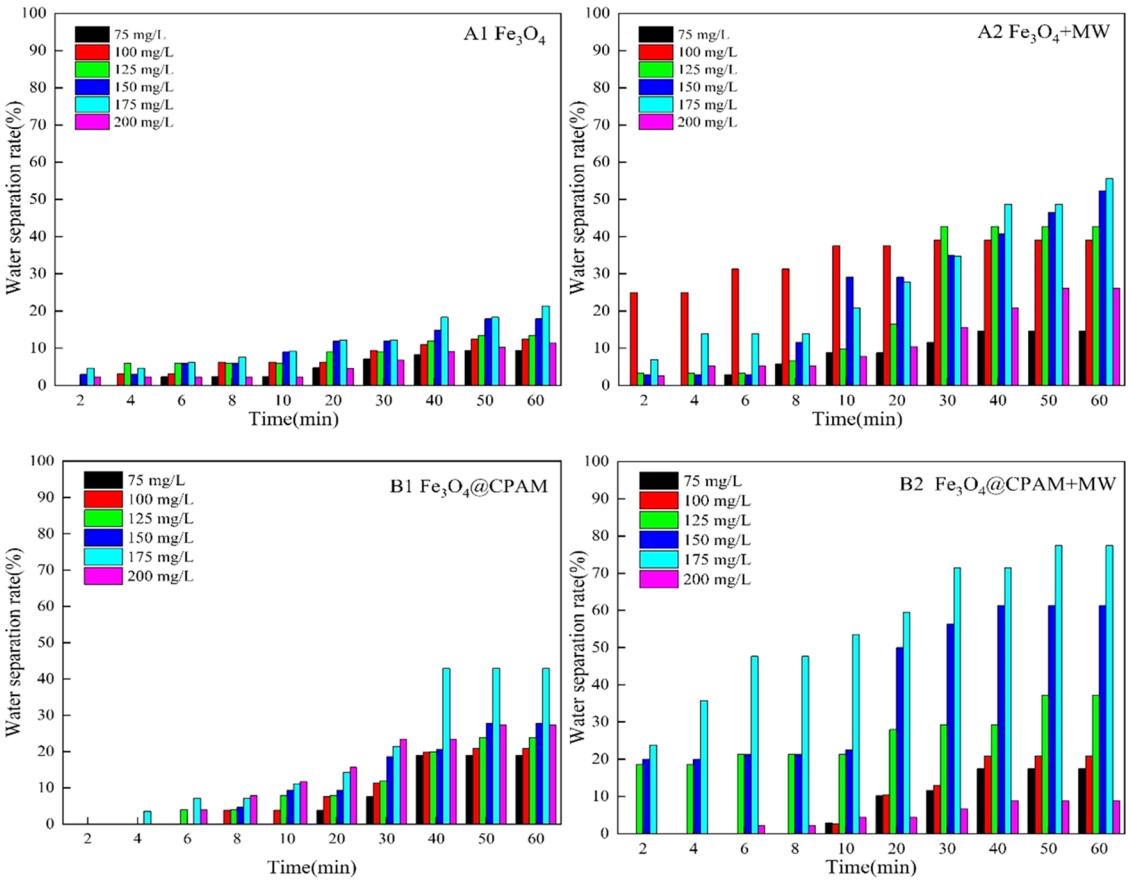

Figure 17. Influence of the magnetic nanoparticle concentration on the demulsification.

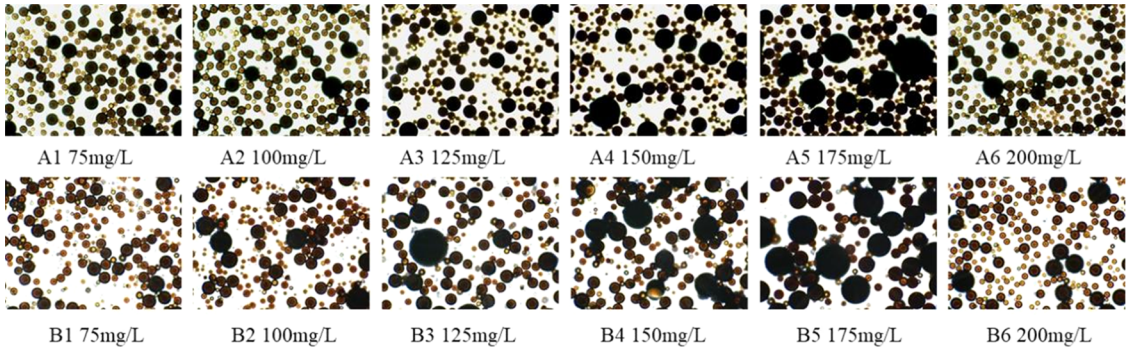

Figure 18. Influence of magnetic Fe_3O_4@CPAM nanoparticle concentration on oil droplet distribution with and without microwave irradiation (A1−A6 show the effects of individual magnetic nanoparticles, while B1−B6 show the effects of magnetic nanoparticle−microwave coupling).

42.11°. When the irradiation time increased from 10 to 20 s, the contact angle of Fe_3O_4@CPAM increased from 46.41 to 55.69°. When the irradiation time increased from 30 to 70 s, the contact angle of Fe_3O_4@CPAM decreased from 42.53 to 41.25°. The contact angle of Fe_3O_4@CPAM corresponding to the optimal irradiation time of 20 s reached a maximum value of 55.69°.

As can be seen from the above results, with a prolongation in irradiation time, the contact angle of Fe_3O_4@CPAM initially increased; this was because the hydrogen bonds of water molecules were weakened or partially destroyed by the microwave electromagnetic field, resulting in a decrease in the number of hydrogen bonds.[6] The interaction between molecules was weakened, resulting in the enhancement of the hydrophobic effect of the magnetic nanoparticles, making it easier to replace the original emulsifier molecules and adsorb onto the oil−water interface, finally promoting demulsification. However, if the microwave irradiation time was extended beyond the optimal irradiation time, the Fe_3O_4@CPAM contact angle decreased and its hydrophilicity was enhanced, which was harmful to the adsorption of MNPS on the surface of oil droplets, so the corresponding water separation rate also decreased.

3.5. Effect of the Concentrations of Fe_3O_4 and Fe_3O_4@CPAM on Demulsification. *3.5.1. Demulsification Performance.* The magnetic nanoparticles selected in this study were Fe_3O_4 and Fe_3O_4@CPAM, and their mass concentrations ranged from 75 to 200 mg/L at 25 mg/L intervals. These emulsions with various types and different magnetic nanoparticle concentrations were separately subjected to conventional demulsification and microwave radiation demulsification.

https://doi.org/10.1021/acsomega.3c08238
ACS Omega 2024, 9, 9202−9215

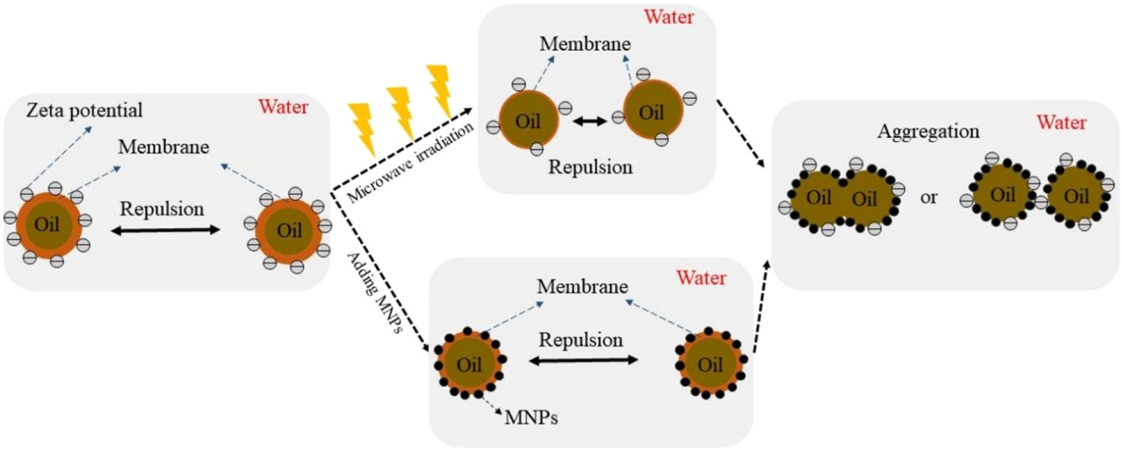

Figure 19. Schematic illustration of the demulsification mechanism of Fe_3O_4@CPAM MNPs.

The microwave irradiation power was 400 W, and the microwave irradiation time was set at 20 s. These experimental results are shown in Figure 17.

It can be seen from Figure 17 that with or without microwave action, an increase in the magnetic nanoparticle concentration resulted in an increase followed by a decrease in the water separation rate. When the Fe_3O_4 concentration was 175 mg/L, the water separation rates of the emulsion for 1 h were 21.34 and 55.56% without and with the action of microwaves, respectively. When the Fe_3O_4@CPAM concentration was 175 mg/L, the water separation rates of the emulsion for 1 h were 42.86 and 77.38% without and with microwave radiation, respectively.

3.5.2. Demulsification Mechanism. 3.5.2.1. Distribution of Oil Droplets. To further elucidate the mechanism of the influence of magnetic nanoparticle concentrations on the coalescence of oil droplets for different demulsification methods, microscopy images of oil droplets were used for the comparative analysis. Fe_3O_4@CPAM powder with the strongest microwave coupling effect was selected as an example. The results are shown in Figure 18.

Figure 18A1−A6 shows that when only magnetic nanoparticles were used, as the concentration of Fe_3O_4@CPAM increased, the oil droplet size first increased and then decreased and the number of oil droplets first became less and then more.

The reasons for the above phenomenon were as follows: (1) In the absence of microwave action, when the concentration of magnetic nanoparticles increased, more magnetic nanoparticles were adsorbed to the oil/water interface to form a mixed film structure. The hybrid film structure reduced the strength of the original interfacial film, leading to the process of contact and collision of droplets with each other, which merged into large droplets (Figure 18A1−A5,18B1−B5).[21] (2) As the concentration of the magnetic polymer increased, the number of polymer molecules adsorbed at the oil−water interface was more, and the electrostatic repulsion of oil droplets was weakened. (3) The magnetic flocculant macromolecular chain can adsorb multiple negatively charged oil beads to form flocs, and precipitation occurs. (4) The higher the concentration of the magnetic flocculant was, the stronger the electric neutralization and sweeping net capture, and the more oil beads were adsorbed and bridged, resulting in the formation of a larger floc structure, and oil−water separation was achieved by gravity. (5) The more electromagnetic energy dissipated by magnetic nanoparticles due to dipolar polarization and ionic conduction under the action of microwaves, the greater the thermal energy was converted, with accelerating Brownian motion of oil droplets and promoting their aggregation. (6) As the concentration of magnetic nanoparticles increases, the electromagnetism of oil droplets was enhanced, and the microwave action leads to an increase in the electromagnetic force between oil droplets.[26] Figure 19 shows a schematic illustration of the demulsification mechanism of Fe_3O_4@CPAM MNPs.

However, after the concentration of magnetic nanoparticles reached 175 mg/L, the droplets decreased and became more numerous (Figure 18A5,A6,B5,B6) when the concentration continued to increase.

This was because the excessive concentration accelerated the agglomeration of magnetic nanoparticles, which was unfavorable for the adsorption of MNPS at the oil−water interface. Additionally, the concentration of magnetic nanoparticles further increased; a particle film structure appeared, increasing the agglomeration required to overcome the energy barrier and blocking the agglomeration that occurs during droplet collision. The bridging flocculation effect was enhance by this particle film, which promoted the formation of a three-dimensional mesh structure in the continuous phase and reduced the chance of contact aggregation between droplets.[26] And as the concentration of magnetic nanoparticles increased, magnetic nanoparticles attracted each other into clusters, reducing the specific surface area of the magnetic nanoparticles, which, in turn, led to a weakening of the attraction of magnetic nanoparticles to emulsifiers and active molecules. At the same time, when the structure of flocs reached a certain level, adding flocculant again would slow or hinder the aggregation between flocs due to electrostatic repulsion.

4. CONCLUSIONS

In this study, a new type of magnetic flocculant, Fe_3O_4@CPAM, was synthesized by a water-soluble method. A heavy oil-in-water emulsion stabilized by 1.50% OP-10 and 0.15% HPAM was used as the research object. The influence laws and mechanisms of microwave radiation powers, microwave radiation times, and magnetic nanoparticle concentrations on synergistic demulsification were systematically analyzed through experiments, and the following conclusions can be obtained. In addition, we found in our experiments that the magnetic nanoparticles before and after the modification were configured as a mother liquor, and the phenomenon of magnetic nanoparticles settling occurred in the beaker after some time of rest; we conjectured that if we

https://doi.org/10.1021/acsomega.3c08238
ACS Omega 2024, 9, 9202−9215

could solve the problem of rapid settling of the magnetic nanoparticles, we could further enhance the emulsification breaking ability of the modified magnetic nanoparticles.

(1) With the increase in microwave radiation power, the water separation rate of the emulsion first increased and then decreased; with the prolongation of microwave radiation time, the water separation rate initially became larger and then smaller.

(2) In the range of optimal radiation parameters, there was a more obvious coupling synergy between microwaves and modified magnetic nanoparticles. This was due to a lower absolute potential of Fe_3O_4@CPAM and its higher hydrophobicity.

(3) With microwave radiation, the increased electromagnetic energy dissipated by magnetic nanoparticles and the enhanced electromagnetism of oil droplets leads to an increase in the water separation rate of the emulsion with increasing magnetic nanoparticle concentration; however, after exceeding a certain concentration, the water separation rate of the emulsion began to decrease.

(4) With the increase in magnetic nanoparticle concentration, the stronger the electric neutralization and sweeping net capture, the more oil beads were adsorbed and bridged, resulting in the formation of a larger floc structure. However, when the concentration of the magnetic flocculant reached 175 mg/L, the surface of the oil beads reached adsorption saturation and no longer provided voids for bridging.

AUTHOR INFORMATION

Corresponding Author

Nana Sun − *College of Petroleum Engineering, Xi'an Shiyou University, Xi'an 710312 Shaanxi, P. R. China*; Email: bingyuxuan6666@126.com

Authors

Huina Sun − *Gas Production Plant No. 1, North China Oil & Gas Branch, North China Petroleum Bureau, Zhengzhou 450000 Henan, P. R. China*

Jianbo Hu − *College of Petroleum Engineering, Xi'an Shiyou University, Xi'an 710312 Shaanxi, P. R. China*; orcid.org/0000-0002-4173-9261

Shiqi Xu − *College of Petroleum Engineering, Xi'an Shiyou University, Xi'an 710312 Shaanxi, P. R. China*

Lisha Shen − *College of Petroleum Engineering, Xi'an Shiyou University, Xi'an 710312 Shaanxi, P. R. China*

Yuli Ma − *College of Petroleum Engineering, Xi'an Shiyou University, Xi'an 710312 Shaanxi, P. R. China*

Complete contact information is available at: https://pubs.acs.org/10.1021/acsomega.3c08238

Notes

The authors declare no competing financial interest.

ACKNOWLEDGMENTS

The authors thank the National Natural Science Foundation of China (Approval No. 51904246), the Xi'an Youth Science and Technology Lifting Project (095920221360), the Shaanxi Provincial Natural Science Foundation (2023-JC-YB-421), and the Shaanxi Provincial Natural Science Foundation (2023-JC-QN-0467) for financial support.

REFERENCES

(1) Tian, G. W.; Chen, Y.; Wang, Y. L.; Zhang, H. Y. Chemical demulsification mechanism and its research progress. *Bull. Chin. Ceram. Soc.* **2018**, *37* (1), 155−159.

(2) Wang, D.; Yang, D. L.; Huang, C.; Huang, Y. Y.; Yang, D. Z.; Zhang, H.; Liu, Q.; Tang, T.; Zeng, H.; et al. Stabilization mechanism and chemical demulsification of water-in-oil and oil-in-water emulsions in petroleum industry: A review. *Fuel* **2021**, *286*, No. 119390.

(3) Sun, N. N.; Jiang, H. Y.; Wang, Y. L.; Qi, A. J. A comparative research of microwave, conventional-heating, and microwave/chemical demulsification of Tahe heavy-oil-in-water emulsion. *SPE Prod. Oper.* **2018**, *33* (02), 371−381.

(4) Lv, X.; Song, Z.; Yu, J.; Su, Y.; Zhao, X.; Sun, J.; Mao, Y.; Wang, W. Study on the demulsification of refinery oily sludge enhanced by microwave irradiation. *Fuel* **2020**, *279*, No. 118417.

(5) Binner, E. R.; Robinson, J. P.; Silvester, S. A.; Kingman, S. W.; Lester, E. H. Investigation into the mechanisms by which microwave heating enhances separation of water-in-oil emulsions. *Fuel* **2014**, *116*, 516−521.

(6) Martínez-Palou, R.; Cerón-Camacho, R.; Chávez, B.; Vallejo, A. A.; Villanueva-Negrete, D.; Castellanos, J.; Karamath, J.; Reyes, J.; Aburto, J. Demulsification of heavy crude oil-in-water emulsions: A comparative study between microwave and thermal heating. *Fuel* **2013**, *113*, 407−414.

(7) Ali, N.; Zhang, B. L.; Zhang, H. P.; Zaman, W.; Li, X. J.; Li, W.; Zhang, Q. Y. Interfacially active and magnetically responsive composite nanoparticles with raspberry like structure; synthesis and its applications for heavy crude oil/water separation. *Colloids Surf., A* **2015**, *472*, 38−49.

(8) Liang, J. L.; Du, N.; Song, S.; Hou, W. G. Magnetic demulsification of diluted crude oil-in-water nanoemulsions using oleic acid-coated magnetite nanoparticles. *Colloids Surf., A* **2015**, *466*, 197−202.

(9) Xu, H. Y.; Jia, W. H.; Ren, S. L.; Wang, J. Q. Novel and recyclable demulsifier of expanded perlite grafted by magnetic nanoparticles for oil separation from emulsified oil wastewaters. *Chem. Eng. J.* **2018**, *337*, 10−18.

(10) Zhao, H. T.; Zhang, C.; Qi, D. M.; Lu, T.; Zhang, D. One-step synthesis of polyethylenimine-coated magnetic nanoparticles and its demulsification performance in surfactant-stabilized oil-in-water emulsion. *J. Dispersion Sci. Technol.* **2019**, *40* (2), 231−238.

(11) Cui, H. C.; Li, D. C.; Zhang, Z. L. Preparation and characterization of Fe_3O_4 magnetic nanoparticles modified by perfluoropolyether carboxylic acid surfactant. *Mater. Lett.* **2015**, *143*, 38−40.

(12) Sadeghi, S. S.; Azhdari, H.; Arabi, H.; Moghaddam, A. Z. Surface modified magnetic Fe_3O_4 nanoparticles as a selective sorbent for solid phase extraction of uranyl ions from water samples. *J. Hazard. Mater.* **2012**, *215*−*216*, 208−216.

(13) Wang, J. P.; Chen, Y. Z.; Ge, X. W.; Yu, H. Q. Gamma radiation-induced grafting of a cationic monomer onto chitosan as a flocculant. *Chemosphere* **2007**, *66* (9), 1752−1757.

(14) Li, J.; Chen, C. L.; Zhao, Y.; Hu, J.; Shao, D. D.; Wang, X. K. Synthesis of water-dispersible Fe_3O_4@β-cyclodextrin by plasma-induced grafting technique for pollutant treatment. *Chem. Eng. J.* **2013**, *229*, 296−303.

(15) Raj, P.; Batchelor, W.; Blanco, A.; Fuente, E. D. L.; Negro, C.; Garnier, G. Effect of polyelectrolyte morphology and adsorption on the mechanism of nanocellulose flocculation. *J. Colloid Interface Sci.* **2016**, *481*, 158−164.

(16) Shao, Y. H. Preparation and Application of Novel Cationic Polyacrylamide "Water-in-Water" Emulsion, Thesis; South China University of Technology: 2020.

(17) Li, X.; Zheng, H. L.; Gao, B. Y.; Sun, Y. J.; Liu, B. Z.; Zhao, C. L. UV-initiated template copolymerization of AM and MAPTAC: microblock structure, copolymerization mechanism, and flocculation performance. *Chemosphere* **2017**, *167*, 71−81.

(18) Zhang, L. X. A Study on Synergistic Demulsification of Microwave-Magnetic Nanoparticle, Thesis; Xi'an Shiyou University: 2020.

https://doi.org/10.1021/acsomega.3c08238
ACS Omega 2024, 9, 9202−9215

(19) Jin, K. B. Study on the Microwave-Chemical Demulsification Technology in the End Point of the Transportation of the Crude Oil Emulsion, Thesis; Xi'an Shiyou University: 2018.
(20) Deng, S. B.; Bai, R. B.; Chen, J. P.; Yu, G.; Jiang, Z. P.; Zhou, F. S. Effects of alkaline/surfactant/polymer on stability of oil droplets in produced water from ASP flooding. *Colloids Surf., A* **2002**, *211*, 275−284.
(21) Sun, N. N. Research on the Emulsification of the Heavy Crude Oil and Its Demulsification by Microwave Chemical Method, Thesis; Southwest Petroleum University: 2016.
(22) Chen, Y.; Tian, G. W.; Liang, H. B.; Liang, Y. N. Synthesis of magnetically responsive hyperbranched polyamidoamine based on the graphene oxide: Application as demulsifier for oil-in-water emulsions. *Int. J. Energy Res.* **2019**, *43* (9), 4756−4765.
(23) Ghanbari, M.; Esmaeilzadeh, F. Demulsification by increasing the gravitational force acting upon the dispersed phase owing to the adsorption/absorption of the magnetite particles. *J. Dispersion Sci. Technol.* **2019**, *40* (11), 1581−1590.
(24) Huang, X. F.; Xion, Y. J.; Lu, L. J.; Liu, J.; Peng, K. M. Manipulation of surface hydrophobicity and charge of demulsifying bacteria using functional magnetic nanoparticles: A mechanistic study of demulsification performance. *Energy Fuels* **2017**, *31* (3), 3295−3304.
(25) Li, S. Y. The Research on Infuence Law of Microwave Frequency Effect on Demulsification, Thesis; Xi an Shiyou University: 2015.
(26) Sun, N. N.; Chang, X. H.; Sun, H. N.; Shen, L. S.; Su, R. Y. Study on the coupling effect of microwave and magnetic nanoparticles on oil droplet coalescence. *SPE J.* **2022**, *27* (5), 3051−3062.

https://doi.org/10.1021/acsomega.3c08238
ACS Omega 2024, 9, 9202−9215